Slot-Fed Higher Order Mode Fabry–Perot Filters

James McCleary, *Student Member, IEEE,* Ming-yi Li, and Kai Chang, *Fellow, IEEE*

Abstract—**Low loss bandpass filters consisting of Fabry–Perot resonators excited by waveguide fed slots coupling to higher order resonator modes are demonstrated. For close reflector spacings, the waveguide couples efficiently through the slots to the TEM_{400} and TEM_{300} modes. The characteristics of both rectangular and circular waveguide feeds with various slot lengths and widths are presented. At X-band the filters have unloaded Q values which range from 1000 to 7000 with insertion losses less than 1 dB. The filters which have the rectangular waveguide feeds are mechanically tunable over a 20% bandwidth.**

I. Introduction

THIS PAPER presents results on efficient coupling to the higher order modes of a Fabry–Perot resonator through slots fed by waveguide. The problem of coupling to a mode of a Fabry–Perot resonator is essentially that of coupling to a propagating beam within the resonator. Most previous work in this area has been in coupling to a fundamental Gaussian beam. A good way to couple from waveguide to a Gaussian beam is through a horn, the most efficient being a corrugated horn [1]. Once launched from a horn, a Gaussian beam can be coupled into a resonator through metal grids or dielectric plates for such applications as diplexing and filtering [2]–[6].

A popular coupling method used in the characterization of dielectrics is from waveguide through small holes [7], [8]. This method of coupling to a fundamental mode is not very efficient, but the objective of this application is not to achieve good coupling, but rather a high Q [9]. A single element in general does not couple well to a Gaussian beam. Mink's analysis show that an array of elements is needed to efficiently couple to a fundamental mode of a Fabry–Perot resonator [10].

The literature on the applications of Fabry–Perot resonators to power combining and oscillator stabilization contains various examples of fundamental-mode coupling methods. A few include dielectric tapers, slots, patches, patch-illuminated slots, circular-apertures, and waveguide apertures [11]–[16].

Kuraev *et al.*, have conducted theoretical and experimental analyses of coupling transitions consisting of tapered waveguide sections [17], [18]. Cam *et. al.*, have applied the boundary element method to solve for the current distribution on a reflector of a resonator disturbed by a circular aperture [19].

In [20], the authors reported a low-loss filter consisting of a plano-concave resonator fed by rectangular waveguide through slots. Low loss occurred by coupling to a fundamental mode near the resonant frequency of the slots. In this paper, we report improved filter performance by slot-coupling to higher order modes in concave resonators. The results include mechanically tunable X-band filters with insertion losses less than 1 dB and unloaded Q values ranging from 1000 to 7000. Although our experiments were conducted at X-band, the filters should have many applications at millimeter-wave and submillimeter-wave frequencies where conventional filters have higher losses and lower values of Q.

The rest of the paper is organized as follows. First is a brief review of resonator mode theory. Then follows a description of experimental setups and the results of experiments using rectangular and circular waveguide feeds.

Manuscript received August 18, 1992. This work was supported in part by the Army Research Office and the Department of Defense through a National Defense Science and Engineering Graduate Fellowship.

The authors are with the Department of Electrical Engineering, Texas A&M University, College Station, Texas 77843-3128.

IEEE Log Number 9211928.

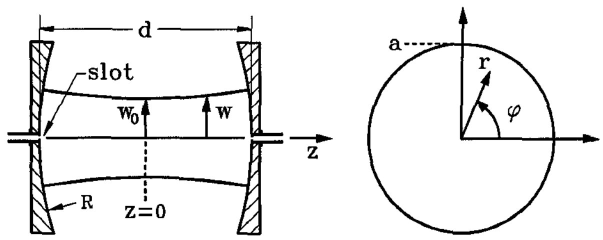

Fig. 1. Concave-concave resonator fed by waveguide through slots. Also shown is the coordinate system. The reflectors have radii of curvature R, have radii a, and are separated by an axial distance d.

II. Resonator Modes

The experiments described in this paper deal with Fabry–Perot resonators configured like the one shown in Fig. 1. This resonator consists of two circular concave reflectors separated by an axial distance d. The reflectors have equal radii of curvature R. Power couples into and out of the resonator through waveguide-fed slots at the center of each reflector.

The resonant frequencies of the resonator in cylindrical coordinates are given by the well known formula [21]

$$f_{plq} = \frac{c}{2d}\left[(q+1) + \frac{1}{\pi}(2p+l+1)\arccos(1-d/R)\right]. \quad (1)$$

The plq are mode numbers. The resonant fields are approximately TEM, and the modes are denoted by TEM_{plq}. Fundamental modes have $p = l = 0$ and have radially symmetric field distributions which are approximately Gaussian. The quantity $(q+1)$ is the number of half-wavelengths of the standing wave set up between the reflectors. The standing wave is formed by the Gaussian beam which propagates back and forth between the reflectors. Illustrated in Fig. 1 is the beam radius w which is the contour where the amplitude of the beam is $1/e$ of its value on the axis. At the center of the

0018-9480/93$03.00

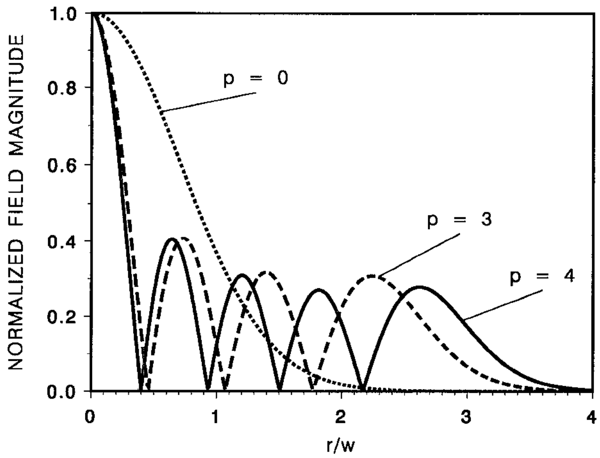

Fig. 2. Ideal transverse field distributions of the TEM_{000} ($p = 0$), TEM_{300} ($p = 3$), and TEM_{400} ($p = 4$) modes.

resonator ($z = 0$ in Fig. 1), the beam has a minimum radius w_0 called the beam waist given by [21]

$$w_0^2 = \frac{\lambda}{2\pi}\sqrt{d(2R-d)}\,. \tag{2}$$

The beam radius at any other location in the resonator is expressed in terms of the waist as [21]

$$w^2(z) = w_0^2\left[1 + \left(\frac{\lambda z}{\pi w_0^2}\right)^2\right]. \tag{3}$$

In particular, the beam incident on a reflector (at $z = \pm d/2$) has radius w_r given by

$$w_r^2 = \frac{\lambda R}{\pi}\sqrt{\frac{d}{2R-d}}\,. \tag{4}$$

The mode numbers p and l describe higher order modes which have nulls along contours of constant r and ϕ, respectively. The higher order modes for which $l \neq 0$ have a null along the resonator axis ($r = 0$). Since the slots in Fig. 1 are along the axis, coupling to these modes is weak [8].

The transverse fields of the modes for which $l = 0$ but $p \neq 0$ have radially symmetric distributions given approximately by the product of Gaussian and Laguerre functions. The magnitudes of these distributions are given by [21]

$$u(r) = \frac{w_0}{w}\exp\left(-\frac{r^2}{w^2}\right)\left|L_p\left(2\frac{r^2}{w^2}\right)\right|, \tag{5}$$

where L_p is a Laguerre polynomial. An expression for the Laguerre polynomials is [22]

$$L_p(x) = \sum_{m=0}^{p}(-1)^m\frac{p!}{(p-m)!\,m!\,m!}x^m\,. \tag{6}$$

Of particular interest in this paper are the TEM_{300} and TEM_{400} modes. Fig. 2 shows the transverse fields for these modes as well as the fundamental mode ($p = 0$). They are plotted as functions of the radial coordinate r normalized by the beam radius w.

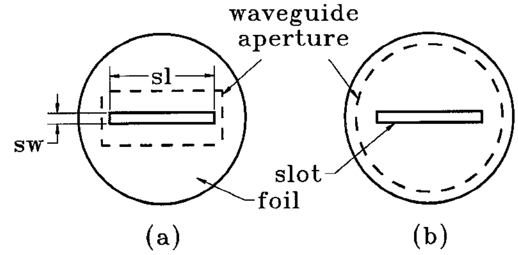

Fig. 3. Dimensions and positions of the slots for (a) the rectangular waveguide feed and (b) the circular waveguide feed. The slots have width sw and length sl.

III. Measurement Setups for Slot-Fed Filters

Measurements of the resonator included testing of both rectangular and circular waveguide feeds at X-band frequencies. Fig. 1 shows the general experimental setup for both feeds. The rectangular waveguide feed is standard 0.9″ × 0.4″ (22.9 mm × 10.2 mm) X-band waveguide. For the measurements with the circular waveguide feed, transitions from rectangular to circular waveguide were used. The diameter of the circular waveguide output of each transition is 27.79 mm. The transition contains mode filters which allow single dominant mode operation with good performance from 10.5 GHz to 11.7 GHz. Each feed is mounted flush to a reflector. The other end of each feed is connected by coax to an HP8510 network analyzer.

The reflectors are two aluminum discs which have 9″ (22.9 cm) diameters and 40″ (101.6 cm) radii of curvature. A plug of 3″ (7.62 cm) diameter is removable from the center of each reflector. The plugs allow different feed structures to be tested without manufacturing entirely different reflectors. Cut through the center of each plug is a waveguide aperture which matches the dimensions of the waveguide feed. The reflectors are mounted on an optical rail which allows measurement of distance accurate to 0.1 mm.

Coupling from the waveguides to the resonator is through slots cut in copper or brass foil. Fig. 3 shows the general dimensions of the slots. The slots are sw wide and sl long. Their orientation is orthogonal to the direction of the dominant mode electric field in each guide. Tape fixes the slots over the waveguide apertures.

TRL calibrations were made to set the reference planes for S-parameter measurements at the ends of the waveguide feeds. This means that unloaded Q measurements were not of the resonator by itself, but of the resonator loaded by the slots.

IV. Rectangular Waveguide Slot-Fed Filters

The measurements of rectangular waveguide slot-fed filters include two slot sizes: 0.5 mm × 23 mm and 0.5 mm × 20 mm. The 23 mm long slot extends across the width of the waveguide. Other slots with larger widths were also tested, but only the 0.5 mm wide slots provided consistently good isolation ($\geq$ 20 dB) between adjacent modes across the 8–12 GHz measurement band. We use isolation to refer loosely to the difference between the strength of a peak of a resonance and the floor between it and an adjacent resonance. For example, consider Fig. 4 which shows an S_{21} measurement

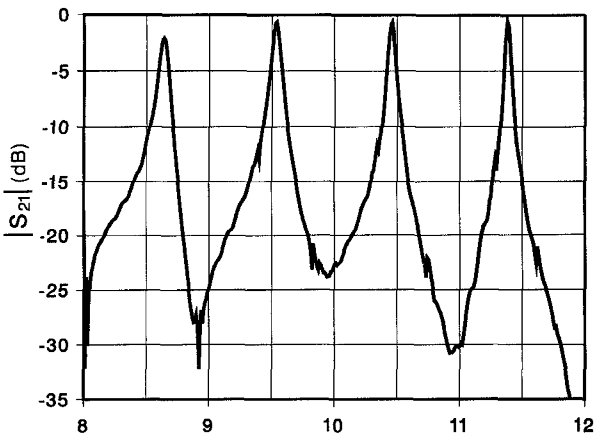

Fig. 4. S_{21} measurement of the rectangular waveguide slot-fed filter for a reflector spacing $d = 20.9$ mm. The modes from left to right are the TEM_{100}, TEM_{200}, TEM_{300}, and TEM_{400} modes.

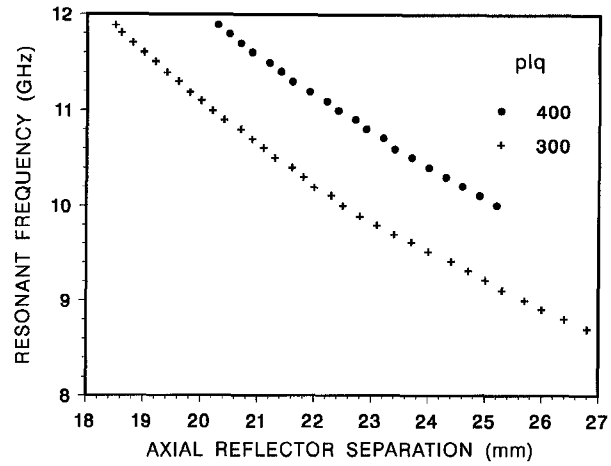

Fig. 5. Measured resonant frequencies versus reflector separation for the rectangular waveguide feed with the 0.5 mm × 23 mm slots.

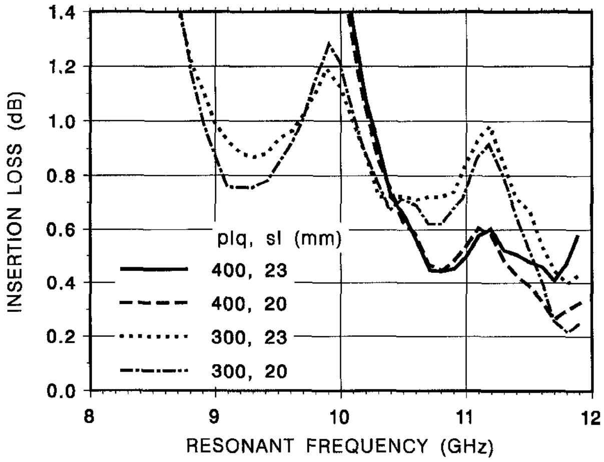

Fig. 6. Insertion loss versus resonant frequency for the rectangular waveguide slot-fed filters.

of the resonator with the 23 mm long slots for a reflector spacing of $d = 20.9$ mm. The modes from left to right are the TEM_{100}, TEM_{200}, TEM_{300}, and TEM_{400} modes. The isolation between the TEM_{300} and TEM_{400} modes is about 30 dB, but the isolation between the TEM_{200} and TEM_{300} modes is less than 25 dB.

All the modes in Fig. 4, including the TEM_{000} fundamental not shown in the figure, exhibited some very low loss behavior (< 1 dB) over the 8–12 GHz band. The TEM_{300} and TEM_{400} modes, however, more consistently had low loss, and they had better isolation from surrounding modes. The following results are for these two modes. Note that these results are only for the TEM_{300} and TEM_{400} modes and not the TEM_{30q} and TEM_{40q} modes in general. The diffraction losses of these modes for $q > 0$ were large.

Fig. 5 shows measured resonant frequencies as a function of reflector separation for the TEM_{300} and TEM_{400} modes with the 23 m long slots. The curves show the mechanical tunability of the filters. The case for the 20 mm long slots has a plot nearly identical to this one. For both cases, the measured frequencies are consistently 2.5–3.5% greater than the theoretical frequencies predicted by (1). One reason for this difference could be strong coupling from the waveguides to the resonator. Another possible explanation is the breakdown of Gaussian beam theory for reflector separations less than one wavelength.

Fig. 6 plots insertion loss against resonant frequency for the four combinations of modes and slot lengths: $p = 4$, $sl = 23$ mm; $p = 4$, $sl = 20$ mm; $p = 3$, $sl = 23$ mm; and $p = 3$, $sl = 20$ mm. Note that each point in the graph represents a different reflector separation, just as in Fig. 5. The TEM_{400} mode has less than 1 dB loss above 10.2 GHz. The TEM_{300} mode has less than 1 dB loss above 9 GHz except for a band between 9.6 and 10.1 GHz. The filters are mechanically tunable over a 20% bandwidth with less than 1 dB insertion loss. From these measurements, the loss does not seem to significantly depend on the slot length. The VSWR for these measurements never exceeded 1.3. The insertion loss is then due mostly to ohmic loses, diffraction, and radiation from the slots which does not couple to the resonator mode.

Fig. 2 can provide a qualitative sense of how diffraction loss affects the insertion loss of the filters. A point at $r/w = a/w_r$ (where a is the reflector radius, and w_r is the beam radius at a reflector given by (4)) represents the incident field at the edge of a reflector. Any field before this point is contained within the resonator; any field above this point is lost to diffraction. Table I shows four of these points which correspond to measurements with the 23 mm long slots. In each row of the table, the first column shows the mode of the measurement (TEM_{400} or TEM_{300}), and the second and third columns contain a measured frequency-reflector separation $(f - d)$ data pair. The fourth column shows the reflector edge point, a/w_r, calculated from (4) using the measured f and d. The fifth column shows the measured insertion loss. The first and second rows of the table show the edge points for the two modes at about 11.9 GHz. Both of the fields which correspond to these points in Fig. 2 have almost converged to zero before these points; the diffraction loss can be expected to be small. The third and fourth rows are measurements of each mode at larger reflector separations where the insertion loss

TABLE I
REFLECTOR EDGE POINTS (a/w_r) FOR THE RECTANGULAR WAVEGUIDE SLOT-FED FILTERS ($sl = 23$ mm)

plq	f (GHz)	d (mm)	a/w_r	L (dB
400	11.8895	20.3	4.0	0.58
300	11.8845	18.5	4.1	0.43
400	10.1085	24.9	3.5	1.32
300	8.8025	26.4	3.2	1.22

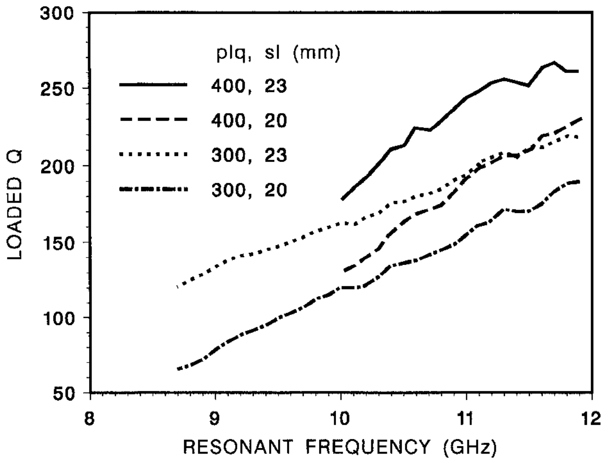

Fig. 7. Q_l versus resonant frequency for the rectangular waveguide slot-fed filters.

exceeds 1 dB. At greater separation (corresponding to lower frequencies) the insertion loss increases rapidly. The fields which correspond to these points in Fig. 2 are just beginning to extend beyond the edges of the reflectors.

This discussion of diffraction loss is very heuristic. The actual fields in the filters are probably not exactly like the ideal fields depicted in Fig. 2. The most that can be said is that diffraction loss limits the tuning bandwidths of the filters. At higher frequencies, the reflectors could easily be made larger in terms of wavelength to improve the performance of the filters.

Fig. 7 shows the loaded $Q(Q_l = f_o/\Delta f_{3\text{dB}})$ versus resonant frequency for the four mode and slot combinations. Although Fig. 6 shows no significant dependence of loss on slot length, Fig. 7 shows a definite dependence of Q_l on slot length. The longer slot has a higher loaded Q (narrower 3 dB bandwidth) than the shorter slot for the same mode and frequency. In addition, the TEM_{400} mode has a higher Q_l than the TEM_{300} mode for either slot or the measured frequencies.

The lower loaded Q of the modes for the 20 mm long slot cases means that the isolation between the modes is less for them also. The isolation between the TEM_{400} and the TEM_{300} modes is always greater than 25 dB for the longer slot but only greater than 20 dB for the shorter slot. Similarly, the isolation between the TEM_{300} and the TEM_{200} modes is greater than 20 dB for the longer slot (for the measured frequencies) but less than 20 dB for the shorter slot for frequencies below 9.3 GHz.

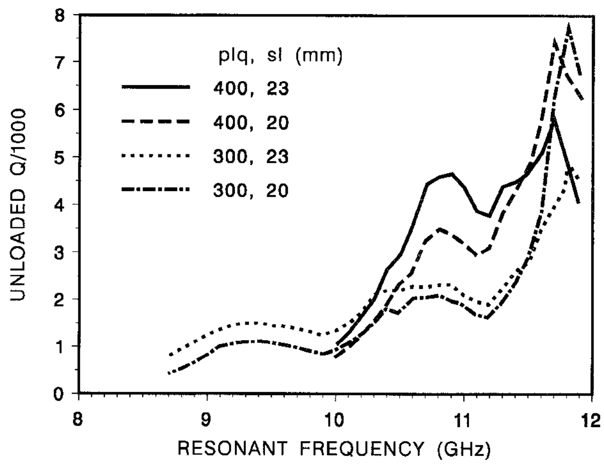

Fig. 8. Q_u versus resonant frequency for the rectangular waveguide slot-fed resonators loaded by the slots.

Fig. 8 shows the unloaded Q as a function of frequency for the four cases. The unloaded Q is given by [23]

$$Q_u = \frac{Q_l}{1 - 10^{-L/20}}, \tag{7}$$

where L is the insertion loss in dB. The relationships between the cases are similar to those for Q_l; however, Q_u does not show the fairly linear dependence on frequency that Q_l shows in Fig. 7. Q_u has a more erratic dependence due to the oscillating frequency response of the loss shown in Fig. 6. The unloaded Q values of the TEM_{300} and TEM_{400} modes for the 20 mm long slot exceed 7000 above 11.5 GHz. Note that Q_u is not for the resonator itself, but of the resonator loaded by the slots.

V. Circular Waveguide Slot-Fed Filters

The rectangular to circular waveguide transitions limited the circular waveguide slot-fed filter measurements from 10.5 to 11.7 GHz, a much narrower band compared to the rectangular waveguide feed case. These measurements also used slots with different widths, rather than lengths. Three slots were tested; all had lengths of 20 mm and widths of 1, 2, and 3 mm, respectively.

As with the rectangular waveguide slot-fed filters, the TEM_{300} and TEM_{400} modes showed better performance in terms of low loss than any other modes. S-parameter measurements for the six combinations of mode and slot width were made at increments of 100 MHz across the 10.5–11.7 GHz band. As with the rectangular waveguide feed, the measured frequencies were an average of about 3% higher than the theoretical frequencies given by (1).

Figs. 9 and 10 show measurements of insertion loss as functions of resonant frequency for the TEM_{400} and TEM_{300} modes, respectively. Each graph contains measurements for each of the three slot widths. From Fig. 9, the TEM_{400} modes are mechanically tunable with less than 0.8 dB loss from 10..6 to 11.6 GHz. Fig. 11 superimposes the S_{21} measurements of the TEM_{400} mode with the 1 mm wide slots for seven different reflector spacings. Similarly, Fig. 10 shows that the loss for the TEM_{300} mode is less than 1 dB except from about 11.1 to

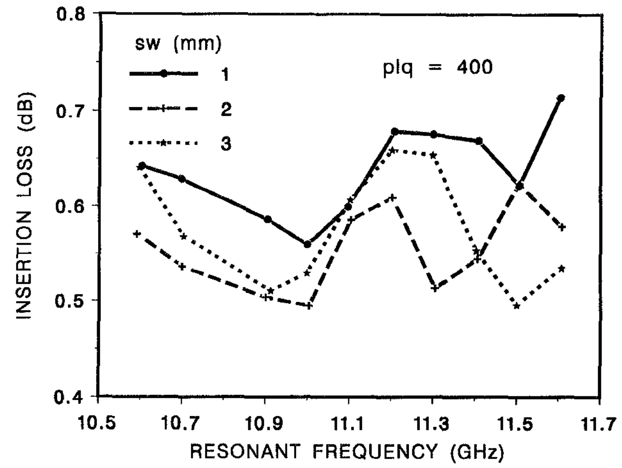

Fig. 9. Insertion loss versus resonant frequency for the circular waveguide slot-fed filters for the TEM_{400} mode.

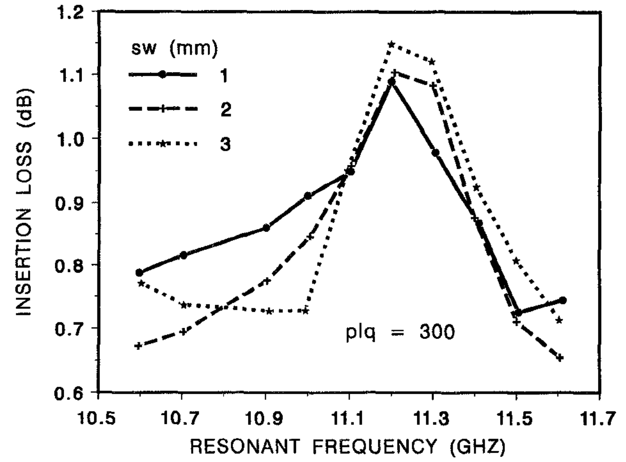

Fig. 10. Insertion loss versus resonant frequency for the circular waveguide slot-fed filters for the TEM_{300} mode.

11.4 GHz. The shapes of the loss curves in Figs. 9 and 10 are similar to the loss curves over the same frequencies in Fig. 6 for the rectangular waveguide case. Also as with the slot length of the rectangular waveguide feed, no direct correlation can be made about the effect of slot width on loss from the data in these figures. One obvious difference between the two different feeds, however, is that the insertion loss of the TEM_{300} mode around 11.2 GHz for the filters with the circular waveguide feed is greater than 1 dB but less than 1 dB for the filters with the rectangular waveguide feed.

The statement that the TEM_{400} mode is tunable with low loss from 10.6 to 11.6 GHz is not entirely true. From about 10.78 to 10.81 GHz, the modes distort, as shown in Fig. 12 for the TEM_{300} mode with the 2 m wide slots. This phenomenon occurred for both modes for all slot widths, but it did not occur for the rectangular waveguide feeds. All measurements in this section are missing a data point at 10.8 GHz due to this distortion.

The loaded Q values of the circular waveguide slot-fed filters have a linear behavior similar to the rectangular waveguide slot-fed filters. Table II shows Q_l for the circular waveguide case by listing the minimum Q_l at 10.6 GHz and the maximum

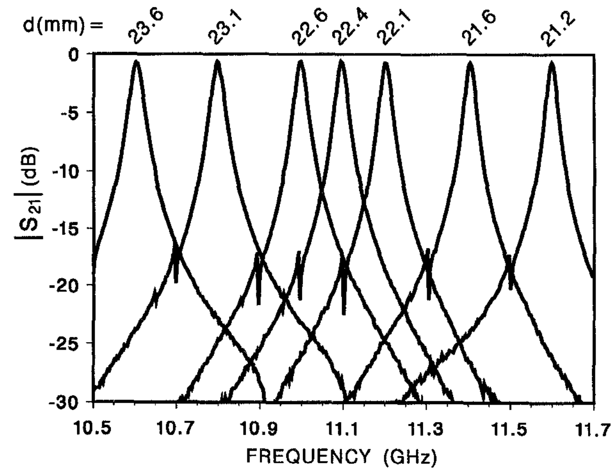

Fig. 11. S_{21} measurements of the circular waveguide slot-fed filter for the TEM_{400} mode with the 1 mm × 20 mm slots. The measurements are for 7 different reflector separations and are superimposed on each other.

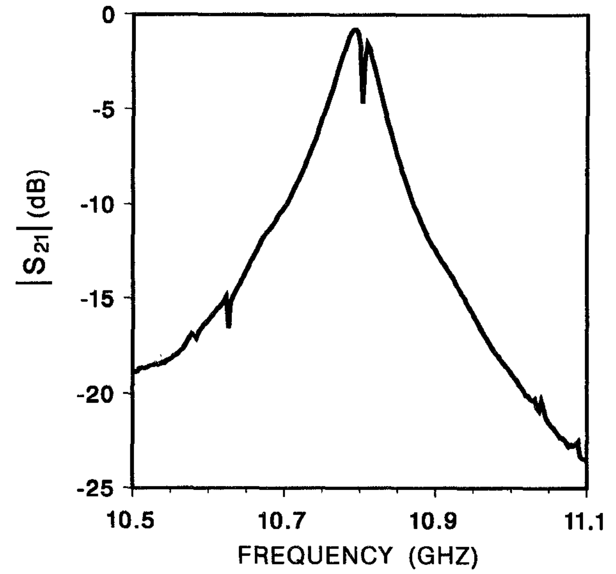

Fig. 12. S_{21} measurement of the circular waveguide slot-fed filter showing distortion for the TEM_{300} mode at 10.8 GHz. The measurement was taken with the 2 m × 20 mm slots and $d = 20.8$ mm.

Q_l at 11.6 GHz for each combination of mode and slot width. The loaded Q decreases with increasing slot width, and for a given slot size, the TEM_{400} mode has a higher Q_l than the TEM_{300} at the same frequency. Both the 1 mm and 2 mm slots for both modes have a higher Q_l than any of the measurements over the same frequency range for the rectangular waveguide case shown in Fig. 8. This means that the circular waveguide slot-fed filters generally have better isolation between adjacent modes than the rectangular waveguide ones. The isolation is typically at least 30 dB for the TEM_{400} mode and at least 25 dB for the TEM_{300} mode for all the slot widths. Figures 13 and 14 show the unloaded Q-factors for the resonator loaded by the slots. The 1 mm wide slot cases for both modes have higher Q_u values than the corresponding cases for the rectangular waveguide shown in Fig. 8.

For both the circular and rectangular waveguide feeds, the TEM_{400} and TEM_{300} modes have less loss than the

TABLE II
LOADED Q VALUES FOR THE CIRCULAR WAVEGUIDE SLOT-FED FILTERS

	$plq = 400$		$plq = 300$	
sw (mm)	Q_l (10.6 GHz)	Q_l (11.6 GHz)	Q_l (10.6 GHz)	Q_l (11.6 GHz)
1	335	452	272	398
2	209	307	183	250
3	152	220	135	194

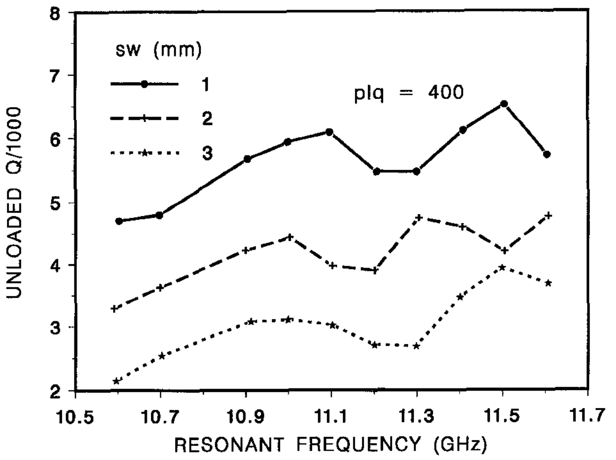

Fig. 13. Q_u versus resonant frequency for the circular waveguide slot-fed resonators loaded by the slots for the TEM_{400} mode.

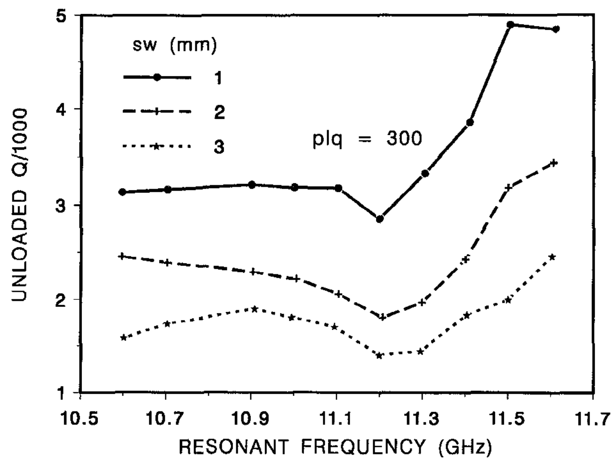

Fig. 14. Q_u versus resonant frequency for the circular waveguide slot-fed resonators loaded by the slots for the TEM_{300} mode.

fundamental TEM_{000} and TEM_{001} modes. The reason for this does not appear to be from diffraction losses because the fields of the fundamental modes are more concentrated around the resonator axis. The higher order resonator modes seem to couple better to the waveguide modes. Fig. 2 shows that the width of the main field distribution of the higher order modes is narrower than the distribution of the fundamental mode. The narrower lobe of a higher order mode may present a better "match" to the waveguide fields than the broader distribution of the fundamental.

VI. CONCLUSIONS

We have demonstrated X-band Fabry–Perot filters which use slots to efficiently couple dominant waveguide modes to the TEM_{400} and TEM_{300} of the resonators. Various slot sizes can be used with both rectangular and circular waveguide feeds to design filters that have unloaded Q values ranging from 1000 to 7000 and insertion losses less than 1 dB. Additional analysis is required to predict the resonant frequencies of the filters as the traditional analytical formula does not predict them accurately enough.

REFERENCES

[1] P. F. Goldsmith, T. Itoh, and K. D. Stephan, "Quasi-optical techniques," in *Handbook of Microwave and Optical Components,* K. Chang, Ed., vol. 1, New York: Wiley, 1981, pp. 344–363.

[2] J. J. Gustuncic, "A quasi-optical receiver design," in *IEEE MTT-S Int. Microwave Symp. Dig.,* pp. 9–101, 1977.

[3] J. A. Arnaud, A. A. M. Saleh, and J. T. Ruscio, "Walk-off effects in Fabry–Perot diplexers," *IEEE Trans. Microwave Theory Tech.,* vol. MTT-22, no. 5, pp. 486–493, May 1974.

[4] H. P. Pickett and A. E. T. Chiou, "Folded Fabry–Perot quasi-optical ring resonator diplexer: theory and experiment," *IEEE Trans. Microwave Theory Tech.,* vol. MTT-31, no. 5, pp. 373–380, May 1983.

[5] P. G. Wannier, J. A. Arnaud, F. A. Pelow, and A. A. M. Saleh, "Quasioptical band-refection filter at 100 GHz," *Rev. Sci. Instr.,* vol. 47, pp. 55–58, 1976.

[6] N. Nakajima and R. Watanbe, "A quasi-optical circuit technology for short-millimeter-wavelength multiplexers," *IEEE Trans. Microwave Theory Tech.,* vol. MTT-29, no. 9, pp. 897–905, Sept. 1981.

[7] A. L. Cullen, "Millimeter-wave open resonator techniques," *Infrared and Millimeter Waves,* Academic Press, vol. 10, ch. 4, pp. 233–281, 1983.

[8] R. G. Jones, "Precise dielectric measurements at 35 GHz using an open resonator," *Proc. Inst. Elec. Eng.,* vol. 123, no. 4, pp. 285–290, Apr. 1976.

[9] A. L. Cullen and P. K. Yu, "The accurate measurement of permittivity by means of an open resonator," *Proc. R. Soc. Lond.,* Series A, vol. 325, pp. 493–509, 1971.

[10] J. W. Mink, "Quasi-optical power-combining of solid-state millimeter-wave sources," *IEEE Trans. Microwave Theory Tech.,* vol. MTT-34, no. 2, pp. 273–279, Feb. 1986.

[11] L. Wandinger and V. Nalbandian, "Millimeter-wave power combining using quasi-optical techniques," *IEEE Trans. Microwave Theory Tech.,* vol. MTT-31, no. 2, pp. 189–193, Feb. 1983.

[12] J. E. Ge, S. F. Li, and Y. Y. Chen, "Millimetre wave quasioptical power combiner," *Electron. Lett.,* vol. 27, no. 10, pp. 880–882, May 1991.

[13] S. Young and K. D. Stephan, "Stabilization and power combining of planar microwave oscillators with an open resonator," in *IEEE MTT-S Int. Microwave Symp. Dig.,* pp. 185–188, 1987.

[14] P. G. Payne and J. Potter, "Efficient power transfer through small apertures," *Electron. Lett.,* vol. 26, no. 25, pp. 2070–2073, Dec. 1990.

[15] E. R. Brown, C. D. Parker, K. M. Molvar, and K. D. Stephan, "A quasioptically stabilized resonant-tunneling-diode oscillator for the millimeter- and submillimeter-wave regions," *IEEE Trans. Microwave Theory Tech.,* vol. MTT-40, no. 5, pp. 846–850, May 1992.

[16] M. Nakayama, M. Heide, T. Tanaka, and K. Mizuno, "Millimeter and submillimeter wave quasi-optical oscillator with multi-elements," in *IEEE MTT-S Int. Microwave Symp. Dig.,* pp. 1209–1212, 1990.

[17] A. A. Kuraev, M. P. Natarov, V. N. Rodionova, V. N. Skresanov, A. Y. Slepyan, and G. Y. Slepyan, "Wide-band matching of quasi-optical resonator with single-molded rectangular waveguide," *Proc. 20th European Microwave Conf.,* Budapest, 1990, supplement A4.5.

[18] V. N. Radionova, Y. A. Slepyan, and G. Y. Slepyan, "Oliner models for quasioptical resonator to rectangular waveguide coupling elements," *Electron. Lett.,* vol. 27, no. 16, pp. 1427–1428, Aug. 1991.

[19] H. Cam, S. Toutain, P. Gelin, and G. Landrac, "Study of a Fabry–Perot cavity in the microwave frequency range by the boundary element method," *IEEE Trans. Microwave Theory Tech.,* vol. 40, no. 2, pp. 298–304, Feb. 1992.

[20] J. C. McCleary and K. Chang, "Low-loss quasi-optical open resonator filters," in *IEEE MTT-S Int. Microwave Symp. Dig.,* pp. 313–316, 1991.

[21] H. Kogelnik and T. Li, "Laser beams and resonators," *Proc. IEEE,* vol. 3, no. 10, pp. 1312–1329, Oct. 1966.

[22] U. W. Hochstrasser, "Orthogonal Polynomials," in *Handbook of Mathematical Functions,* M. Abramowitz and I. A. Stegun Eds., New York: Dover, 1970, p. 775.

[23] K. Chang, F. Hsu, J. Berenz, and K. Nakano, "Find optimum substrate thickness for millimeterwave GaAs MMICs," *Microwaves and RF,* pp. 123–126, Sept. 1984.

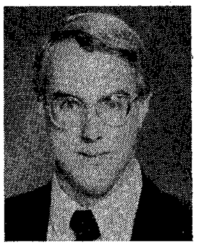

James McCleary was born on September 13, 1966 in New York, NY. He received the B.S. and M.S. degrees in electrical engineering from Texas A&M University in 1988 and 1991, respectively.

In 1986 and 1987 he was a co-op student engineer with the Department of Defense where he worked on digital controls for RF systems. Since 1988 he has been a research assistant at Texas A&M, where he is currently pursuing the Ph.D. degree. His interests are in quasi-optics and the numerical analysis and design of aperture and phase array antenna systems.

He was awarded a National Defense Science and Engineering Fellowship in 1990.

Ming-yi Li received the B.S. and M.S. degrees in electrical engineering from East China Normal University, in 1968 and 1982, respectively.

From 1979 to 1982, he was with the East China Normal University, China, where he was engaged in numerical calculations of electromagnetic fields and scattering problems. In 1982, he joined the Shanghai Research Institute of Microwave Technology, where he was involved in research and development of millimeter-wave devices and circuits. This activity resulted in Ka-band six-port measurement system, Ka-band attenuator, phase shifter, and Ka-band mismatched calibration standard kits. Since 1987, he has been a Research Associated in the Department of Electrical Engineering, Texas A&M University, involved in research on microwave and millimeter-wave circuits, power combining, and measurements.

Mr. Li has published 30 technical papers in microwave and millimeter-wave areas.

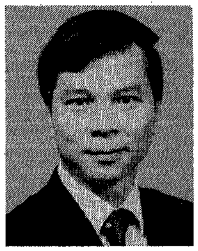

Kai Chang (S'75–M'76–SN'85–F'91) received his B.S.E.E. degree from the National Taiwan University, Taipei, Taiwan; his MS degree from the State University of New York at Stony Brook; and his Ph.D. degree from the University of Michigan, Ann Arbor, in 1970, 1972, and 1976, respectively.

From 1972 to 1976, he worked for the Microwave Solid-State Circuits Group, Cooley Electronics Laboratory of the University of Michigan as a Research Assistant. From 1976 to 1978, he was employed by Shared Applications, Inc., Ann Arbor, where he worked in computer simulation of microwave circuits and microwave tubes. From 1978 to 1981, he worked for the Electron Dynamics Division, Hughes Aircraft Company, Torrance, CA., where he was involved in the research and development of millimeter-wave solid-state devices and circuits, power combiners, oscillators and transmitters. From 1981 to 1985, he worked for the TRW Electronics and Defense, Redondo Beach, CA., as a Section Head, developing state-of-the-art millimeter-wave integrated circuits and subsystems including mixers, VCO's, transmitters, amplifiers, modulators, upconverters, switches, multipliers, receivers, and transceivers. He joined the Electrical Engineering Department of Texas A&M University in August 1985 as an Associate Professor and was promoted to a Professor in 1988. In January 1990, he was appointed E-Systems Endowed Professor of Electrical Engineering. His current interests are in microwave and millimeter-wave devices and circuits, microwave integrated circuits, microwave optical interactions, and antennas.

Dr. Chang served as the editor of the four-volume *Handbook of Microwave and Optical Components* published by John Wiley & Sons, Inc. in 1989 and 1990. He is the editor of the *Microwave and Optical Technology Letters* and the *Wiley Book Series in Microwave and Optical Engineering.* He has published over 180 technical papers and several book chapters in the areas of microwave and millimeter-wave devices and circuits.

Dr. Chang received the Special Achievement Award from TRW in 1984, the Halliburton Professor Award in 1988, the Distinguished Teaching Award in 1989, and the Distinguished Research Award in 1992 from the Texas A&M University.